



Differential Equations of Controlled Pneumatic Actuators for 6-DOF Stewart Platform

B. Andrievsky^{1,2}, D.V. Kazunin^{1,3}, D.M. Kostygova³, N.V. Kuznetsov^{1,4*},
G.A. Leonov^{1,2}, P. Lobanov³, A.A. Volkov¹

¹ *St. Petersburg State University, Russia*

² *Institute for Problems of Mechanical Engineering of RAS, Russia*

³ *Transas Group, Saint Petersburg, Russia*

⁴ *University of Jyväskylä, Finland*

Received: April 6, 2014; Revised: January 27, 2015

Abstract: In the paper, the differential equations of the controlled pneumatic actuators as a part of simulator for training drivers of freight vehicles based on 6-DOF Stewart Platform are presented. The sliding-mode control strategy is proposed and studied by simulations. The experimental results for the existing on-off logical control algorithm are given, showing potential advantage of the sliding-mode controller for tracking fast reference signals.

Keywords: *Stewart platform; control; pneumatic actuator; nonlinear dynamics.*

Mathematics Subject Classification (2010): 00A06, 00A69, 00A72, 03C98, 34L30.

1 Introduction

The present paper is devoted to designing a simulator for training of freight KamAZ vehicle drivers. The simulator is currently under construction by the Transas Co. The car cab is mounted on the Gough–Stewart platform for reproducing the desired motions of the cab. The distinguish feature of the simulator is employing pneumatic servo as actuators.

Pneumatic systems are widely used in many applications, but the control of such systems poses difficult problems due to the nonlinear behavior of friction-like phenomena and great variation of the system properties associated with the system state.

During the last decades, the control/tracking problem for pneumatic actuators has been extensively studied in the literature. The authors of [1] presented results on the

* Corresponding author: <mailto:nkuznetsov239@gmail.com>

modeling and the control of a heavy pneumatic machine designed for handling logs. The paper shows that a significant improvement in performance results from modified self tuning generalized predictive control of pneumatic systems. In [2] it is demonstrated that low friction pneumatic cylinders offer real potential for the precision control systems and the self-tuning strategy is proposed to obtain correct operating parameters at the start of a session. In [2] the low-friction cylinder is compared to conventional, sealed cylinders showing the enhanced performance. An experimental comparison between six different techniques to control the position of a pneumatic actuator, such as PID control, fuzzy control, PID control with pressure feedback, fuzzy control with pressure feedback, sliding mode control and neuro-fuzzy control is given in [3]. It is stressed that the nonlinear nature of pneumatic systems together with the large uncertainty in the model parameters does not allow a realistic comparison using only mathematical models and simulations. The authors conclude that in terms of both error and complexity of design and cost, the Fuzzy logic controller with neural estimator instead of the pressure sensor has some advantages as compared with other control methods. Results of the experimental comparison of PID control and the nonlinear robust tracking control strategy for servo-controlled pneumatic systems are presented in [4], demonstrating some advantages of the proposed nonlinear controller design. A combination of a fuzzy-PID controller used to ensure tracking performance with an adaptable wavelet neuro compensator, used to compensate for the time delay resulting from the control valve is proposed in [5]. By simulation of the linear time delayed model of the pneumatic system, the authors show that the system without delay-time compensation may become unstable when the delay time exceeds 0.02 s, and that the adaptable neural network ensures performance robustness in the face of environment and physical variations. Possibility of chaotic motion in nonlinear systems is discussed in [6].

The paper is organized as follows. The car simulator based on the Stewart platform is briefly described in Section 2, where Gough–Stewart platform construction is recalled, and specifications for control system of the platform are given. The model of the pneumatic actuator is presented in Section 3. The fluid servodrive of the Transas car simulator and the control algorithms are described in Section 4. Results of the simulation and experimental study are given in Section 5. Concluding remarks and the future work intentions are presented in Section 6.

2 Freight Vehicle Simulator Based on Stewart Platform

2.1 Gough–Stewart platform

The *Stewart* (or *Gough–Stewart*) *platform* is a six-degree-of-freedom parallel manipulator. This platform being representative of the class of parallel manipulators, the concepts applicable for it have direct relevance to the entire class [7]. The Stewart platform has 6 degrees of freedom, such as:

- three spatial coordinates: x , y , z ;
- three angular coordinates: yaw ψ , pitch ϑ and roll γ .

Schematic view of the Stewart platform is shown in Fig. 1.

Dynamics of the Stewart platform, arbitrarily placed on six rods of variable length, with allowance for the inertia and weight rods is described as a special case of rigid body motion in [8,9]. The equation of motion of the center of gravity C of the loaded platform

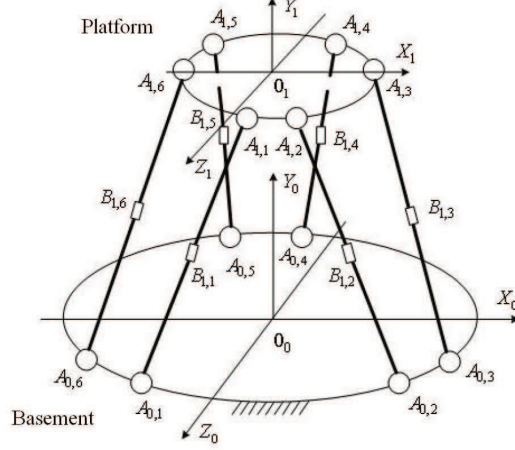


Figure 1: Schematic view of the Stewart platform.

in the fixed reference frame may be written as follows:

$$\begin{aligned} m(\ddot{\mathbf{r}}^0 + \dot{\boldsymbol{\omega}}^0 \times \mathbf{r}_c^0 + \boldsymbol{\omega}^0 \times (\boldsymbol{\omega}^0 \times \mathbf{r}_c^0)) + mg\mathbf{k}_0, \\ \mathbf{r}_c^0 = \mathbf{P} \cdot \mathbf{r}_c, \end{aligned} \quad (1)$$

where $\mathbf{F}^0 = \sum_{k=1}^6 F_k \mathbf{e}_{kt}^0$, F_k ($k = 1, \dots, 6$) are the forces, acting to the platform from the side of the pneumatic actuators, m denotes the mass of the platform with a load, g is the gravity acceleration, $\overrightarrow{OC} = \mathbf{r}_c$ is the radius vector of the center of gravity platform in the moving reference frame, $\ddot{\mathbf{r}}^0$ stands for the acceleration of point O .

The equation of moments with respect to the center of gravity C in the moving reference frame has the following form

$$\begin{aligned} J_c \cdot \dot{\boldsymbol{\omega}} + \boldsymbol{\omega} \times (J_c \cdot \boldsymbol{\omega}) = \mathbf{M}, \\ \mathbf{e}_{kt} = \mathbf{P}^T \cdot \mathbf{e}_{kt}^0, \quad \boldsymbol{\omega} = \mathbf{P}^T \cdot \boldsymbol{\omega}^0, \end{aligned} \quad (2)$$

where $\mathbf{M} = \sum_{k=1}^6 F_k (\mathbf{a}_k - \mathbf{r}_c) \times \mathbf{e}_{kt}$, J_c is the inertia tensor with respect to point C , \mathbf{F}^0 and \mathbf{M} denote the principal forces vector and the principal torque, respectively, acting to the platform from the side of the pneumatic cylinders.

Kinematics of the platform is described by the following matrix equation

$$\mathbf{A} \cdot \mathbf{V}^0 = \dot{\mathbf{l}}, \quad \dot{\mathbf{l}} = (\dot{l}_1, \dots, \dot{l}_6)^T, \quad (3)$$

where matrix \mathbf{A} is composed from the row-vectors

$$\mathbf{L}_k \cdot \mathbf{V}^0 = \dot{l}_k, \quad k = 1, \dots, 6, \quad (4)$$

$(\cdot)^T$ denotes the transpose operation (see [8] for more details).

In the projections on the coordinate axes X, Y, Z , system (1), (2), (3) has the following form:

$$\begin{aligned}
J_x \dot{\omega}_x + (J_z - J_y) \omega_y \omega_z &= \sum_{k=1}^6 F_k (a_{ky} e_{kz} - a_{kz}^* e_{ky}), \\
J_y \dot{\omega}_y + (J_x - J_z) \omega_z \omega_x &= \sum_{k=1}^6 F_k (a_{kz}^* e_{kx} - a_{kx} e_{kz}), \\
J_z \dot{\omega}_z + (J_y - J_x) \omega_x \omega_y &= \sum_{k=1}^6 F_k (a_{kx} e_{kx} - a_{ky} e_{kx}), \\
a_{kz}^* &= a_{kz} - z_c.
\end{aligned} \tag{5}$$

$$\begin{aligned}
m(\ddot{x} + z_c \dot{\omega}_y + z_c \omega_x \omega_z) &= \sum_{k=1}^6 F_k e_{kx} + mg \sin \vartheta, \\
m(\ddot{y} - z_c \dot{\omega}_y + z_c \omega_y \omega_z) &= \sum_{k=1}^6 F_k e_{ky} - mg \cos \vartheta \sin \gamma, \\
m(\ddot{z} - z_c(\omega_x^2 + \omega_y^2)) &= \sum_{k=1}^6 F_k e_{kz} - mg \cos \vartheta \cos \gamma,
\end{aligned} \tag{6}$$

$$\begin{aligned}
\dot{\vartheta} &= \omega_y \cos \gamma - \omega_z \sin \gamma, \\
\dot{\gamma} &= \omega_z + \dot{\psi} \sin \vartheta, \\
\dot{\psi} &= (\omega_y \sin \gamma + \omega_z \cos \gamma) \cdot (\cos \vartheta)^{-1}.
\end{aligned} \tag{7}$$

The system of equations (5)–(7) is of order 12. This system should be supplemented by equations of the external forces F_k ($k = 1, \dots, 6$), acting to the platform from the side of pneumatic actuators.

2.2 Freight vehicle simulator of Transas Co.

The present paper deals with a pneumatically actuated Stewart platform, which serves as a computer-controlled mobile base of the simulator for training of freight KamAZ vehicle drivers. An axonometric plan of the Stewart platform used as a part of the Transas car simulator is presented in Fig. 2.

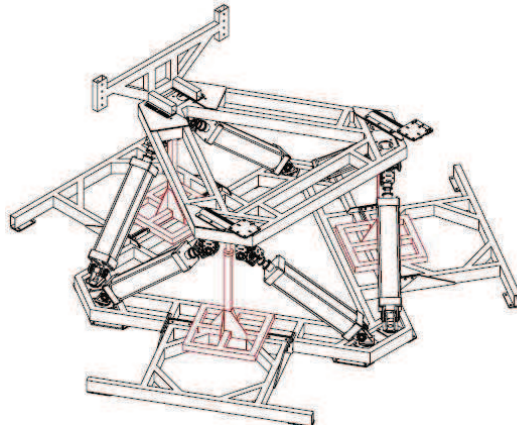


Figure 2: Axonometric plan of the Stewart platform of Transas car simulator.

The considered system peculiarity is the usage of pneumatic servosystems instead of the hydraulic ones. The advantage of pneumatic actuators is the design simplicity and relative ease of operation and maintenance. Besides, they are relatively cheap and functional flexible. As well as the hydraulic systems, they may reproduce forward movement without gears.

Pneumatic actuators have the following advantages over the hydraulic ones:

- Their actuators have higher operating speed and lower cost;

— Return lines are much shorter, since the air can be vented to the atmosphere from any point of the system;

— There is an unlimited supply of air as the working fluid.

However, pneumatic actuators of the same dimension as the hydraulic ones, are producing the smaller force due to the higher fluid pressure in the hydraulic actuators. In addition, it is difficult to ensure sufficient control accuracy by the pneumatic actuators due to the air compressibility. This imposes special requirements to the control system design.

2.3 Specifications for control system of the platform

The control system is aimed at providing prescribed motion of the platform center-of-gravity, and the angular position of the platform, ensuring tracking of the reference signal produced by the higher level of the simulator control. Adaptability of the control system is required for ensuring stable platform behavior in the total region of admissible variables and parameters.

The control algorithm should involve the procedure for converting the input data, removing the platform from the admissible region, to the acceptable one.

The requirements on the tracking precision should be fulfilled by means of minimal frequency of pneumatic valve actuations.

From the experience of the operation of such kind of platforms it is known that, due to leaks in pneumatic equipment, the parasitic oscillations occur in the quiescent state. These oscillations should be suppressed.

Additionally, the control system must ensure fulfillment of the above stated requirements for the case of increasing the mass of the service load up to 400 kg above its nominal value.

3 Pneumatic Actuator Model

3.1 Basic relations

Equations (5)–(7) should be considered jointly with the following equations for pressures p_1 and p_2 in the working and exhaust cavities of the pneumatic cylinder [10, 11]:

$$\dot{p}_1 = \frac{k f_1^{\text{ef}} K p_h \sqrt{RT_h}}{F_1(x_{01} + x)} \varphi(\sigma_1) - \frac{k p_1}{x_{01} + x} \cdot \dot{x}, \quad (8)$$

$$\sigma_1 = p_1/p_h; \quad K = \sqrt{2gk/(k-1)}; \quad x_{01} = V_{01}/F_1;$$

where p_h and T_h denote the air pressure and temperature (respectively) in the header pipe; $f_1^{\text{ef}} = \mu_1 f_1$ is the effective area of the inlet hole; μ_1 denotes the flow coefficient of the inlet pipe; f_1 is the inlet area; x_{01} stands for the initial piston position; V_{01} is the initial working chamber space; k denotes the adiabatic index (for standard air, $k = 1.4$); g is the acceleration of gravity¹. Nonlinear *discharge function* $\varphi(\cdot)$ in (8) has the following form [10, 11]:

$$\varphi(\sigma) = \begin{cases} \sqrt{\sigma^{\frac{2}{k}} - \sigma^{\frac{k+1}{k}}}, & \text{if } 0.528 < \sigma < 1; \\ 0.2588, & \text{if } 0 < \sigma < 0.528. \end{cases} \quad (9)$$

¹ In the present work all the values are given in the engineer's system of units.

Initial values of x_{01} and V_{01} include not only the initial volume of the chamber (the so-called *clearance space*), but also the volume of the pipeline from the distributor to the working cylinder.

Equation for pressure p_2 in the exhaust chamber 2 differs from (8) not only by signs of its members and the piston coordinate, but by the fact that it includes a varying temperature T_2 in the exhaust chamber instead of the constant air temperature T_h in the header pipe:

$$\dot{p}_2 = -\frac{k f_2^{\text{ef}} K \sqrt{RT_2}}{F_2(s + x_{02} - x)} \varphi\left(\frac{\sigma_a}{\sigma_2}\right) + \frac{kp_2}{s + x_{02} - x} \cdot \dot{x}, \quad (10)$$

where $\sigma_2 = \frac{p_2}{p_h}$; $x_{02} = \frac{V_{02}}{F_1}$; $f_2^{\text{ef}} = \mu_2 f_2$, $\varphi(\cdot)$ is given by (9).

Since the adiabatic process occurs in the absence of the heat exchange in the exhaust chamber, the temperature T_2 in (10) may be expressed in terms of p_2 as

$$\frac{p_2}{p_1} = \left(\frac{v_1}{v_2}\right)^k, \quad \frac{p_2}{p_1} = \left(\frac{T_2}{T_1}\right)^{\frac{k}{k-1}}, \quad \frac{T_2}{T_1} = \left(\frac{v_1}{v_2}\right)^{k-1}.$$

Then (10) reads as follows:

$$\dot{p}_2 = -\frac{k f_2^{\text{ef}} K p_2^{\frac{3k-1}{2k}} \sqrt{RT_h}}{F_2(s + x_{02} - x) p_h^{\frac{k-1}{2k}}} \varphi\left(\frac{\sigma}{\sigma_2}\right) + \frac{kp_2}{s + x_{02} - x} \cdot \dot{x}. \quad (11)$$

4 Fluid Servodrive of Transas Car Simulator

4.1 Dynamics model of tracking pneumo actuator

Foregoing equations (5)–(7), (8), (9), (11) make it possible to study motion of the pneumo valve under the variations of the load and the inlet and outlet areas, but these equations do not take into account that input and output cavities are not fixed during the motion control, they may be referred to upper and to lower parts of the pneumatic cylinder, depending on the current control action. Besides, it should be also considered that in the particular servo system, the pressure force is controlled by means of air *exhaust* (not air injection) from the corresponding chamber of the pneumatic cylinder. This is made by means of three controlled outlet valves with different selectional areas, which makes possible to compose the 3-bit control signal (for each direction). Air pressure in the cavities is restored from the surge vessel, which is connected with the compressor, via two uncontrolled valves (one for each chamber). Additionally, in what follows it is taken into account that the weight of the piston is negligibly small in comparison with the load forces applied from the moving platform with the cab, mounted on it.

Following [9, 12], to describe motion of the pneumatic actuator let us introduce the dimensionless controlling parameter $-1 \leq \alpha \leq 1$ such as $f_1 = f_2 = |\alpha| f_{\max}$, where f_{\max} denotes the maximal area of the outlet hole, assuming that if $\alpha > 0$ then the outlet hole of the upper chamber is connected to the atmosphere, and visa versa, if $\alpha < 0$ then this is made for the lower chamber. If $\alpha = 0$ then both chambers are closed off for the air discharge. As is stated above, parameter α is represented by 4 binary digits (one bit is for the sign).

Finally, the following model for air pressures in the chambers is obtained:

$$\begin{aligned} \dot{p}_1 = & \frac{k f_0 K p_h \sqrt{RT_h}}{F_1(x_{01} + x)} \varphi(\sigma_1) - \frac{k p_1}{x_{01} + x} \cdot \dot{x} \\ & - \begin{cases} 0, & \text{if } \alpha > 0, \\ \frac{k f_1^{\text{ef}} K p_1^{\frac{3k-1}{2k}} \sqrt{RT_h}}{F_1(x_{01} + x) p_h^{\frac{k-1}{2k}}} \varphi\left(\frac{p_a}{p_1}\right), & \text{otherwise,} \end{cases} \end{aligned} \quad (12)$$

$$\begin{aligned} \dot{p}_2 = & \frac{k f_0 K p_h \sqrt{RT_h}}{F_2(s + x_{02} - x)} \varphi(\sigma_2) + \frac{k p_2}{s + x_{02} - x} \cdot \dot{x} \\ & - \begin{cases} \frac{k f_2^{\text{ef}} K p_2^{\frac{3k-1}{2k}} \sqrt{RT_h}}{F_2(s + x_{02} - x) p_h^{\frac{k-1}{2k}}} \varphi\left(\frac{p_a}{p_2}\right), & \text{if } \alpha > 0, \\ 0, & \text{otherwise,} \end{cases} \end{aligned} \quad (13)$$

where $K = \sqrt{2gk/(k-1)}$, $x_{01} = V_{01}/F_1$, $x_{02} = V_{02}/F_1$, $f_1 = f_2 = f_{\max}|\alpha|$, $f_1 = f_2 = f_{\max}|\alpha|$, $f_0 = \mu_0 f_{\max}$, $f_1^{\text{ef}} = \mu_1 f_1$, $f_2^{\text{ef}} = \mu_2 f_2$, $\sigma_1 = p_1/p_h$, $\sigma_2 = p_2/p_h$. The first term in (12), (13) describes air feeding the chambers from the compressor over the valve with a sectional area f_0 .

4.2 Sliding-mode control of pneumatic actuator

Let $x^*(t)$ be the reference signal, representing the desired piston position (and, consequently, the running-out of the rod).

To ensure the high tracking accuracy along with robustness to parametric uncertainties, unmodelled nonlinearities and the external disturbances (such as varying forces applied from the load), the following sliding-mode controller may be used [3, 13, 14, 16]:

$$u(t) = e(t) + k_D \dot{e}(t), \quad (14)$$

$$\alpha(t) = \text{sat}\left(\kappa \text{sign}(u) \cdot \sqrt{|u|}\right), \quad (15)$$

where $e(t) = x^*(t) - x(t)$ denotes the tracking error, k_D stands for the damping gain, ensuring ‘‘smooth’’ sliding motion [13–15]. In what follows, after some trial and error iterations, the ‘‘guessed’’ values $k_D = 0.4$ s/m, $\kappa = 15$ have been taken.

5 Simulation and Experimental Results

The simulations of the closed-loop system (12), (13) with sliding-mode controller (14) for all six ‘‘legs’’ of the platform was studied by the simulations. In our study the various reference signals on platform coordinates x_c^* , y_c^* , z_c^* , ψ^* , ϑ^* , γ^* have been converted by means of the kinematic equations (see, e.g. [17]) to the reference signals on the each leg $x_i^*(t)$, $i = 1, \dots, 6$ of the pneumatic servo systems. Then the actual running-out of each rod $x_i(t)$ has been re-converted by means of the inverse kinematic relations [17] to the actual platform coordinates $x_c(t)$, $y_c(t)$, $z_c(t)$, $\psi(t)$, $\vartheta(t)$, $\gamma(t)$ for accuracy evaluation.

One example of the simulation results is demonstrated in Figs. 3–5. The harmonic reference signal on the vertical platform coordinate z_c has been taken, the other reference variables have been taken zeros.

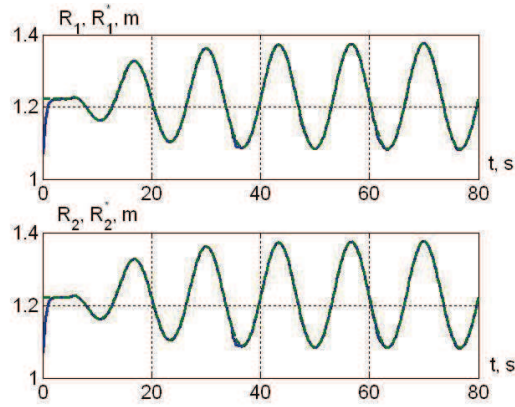


Figure 3: Model (12), (13), controller (14). Legs 1–4 lengths vs t . Solid line – actual value, dashed line – desired value.

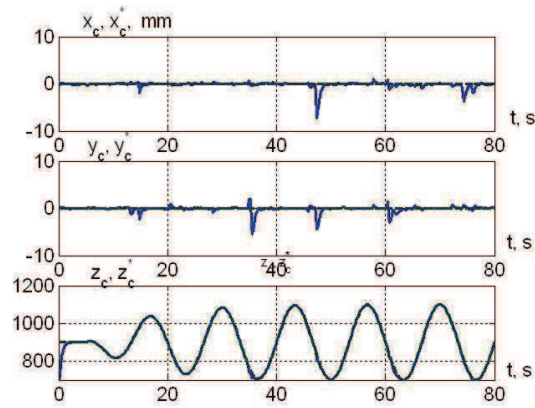


Figure 4: Model (12), (13), controller (14). Platform translational coordinates vs t . Solid line – actual value, dashed line – desired value.

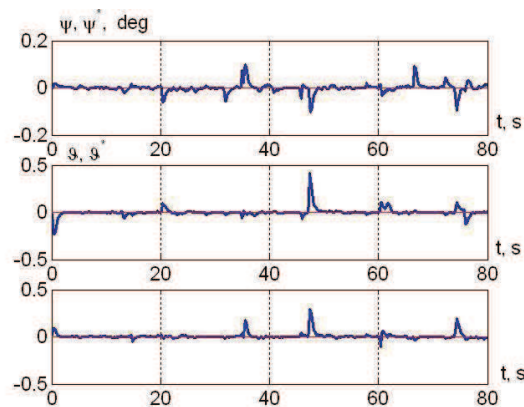


Figure 5: Model (12), (13), controller (14). Platform angular coordinates vs t .

As is seen from the plots, control law (14) ensures high precision and operating speed of tracking process.

The same reference signals have been applied to the real-world set-up (see Fig. 6), which is supplied with the on-off logic controller, which has been borned by the typical solutions for pneumatic automation systems. It is seen from the plots (Figs. 7–9), that the tracking error for the siding mode controller is up to 5 time less than that for the on-off logic controller.



Figure 6: Performing the experiments.

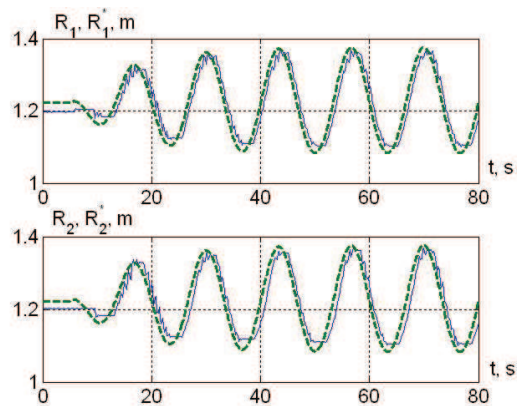


Figure 7: Experimental results. On-off logic control. Legs 1–4 lengths vs t . Solid line – actual value, dashed line – desired value.

6 Conclusions

In the paper the problem of pneumatic actuators control by switching the valves is considered. The actuators are the part of the simulator for training drivers of freight vehicles, based on the 6-DOF Stewart Platform.

The sliding-mode control strategy is proposed and studied by simulations. The experimental results for the existing on-off logical control algorithm are given. Comparison of the results demonstrates possibility for improvement of the stimulator performance based on the sliding-mode controller.

The future work intentions are the implementation of the proposed control law on the real-world pneumatic actuators for experimental valuation of the robustness properties of the sliding-mode controller with respect to the unmodelled plant dynamics, uncertainties and varying external disturbances from the load.

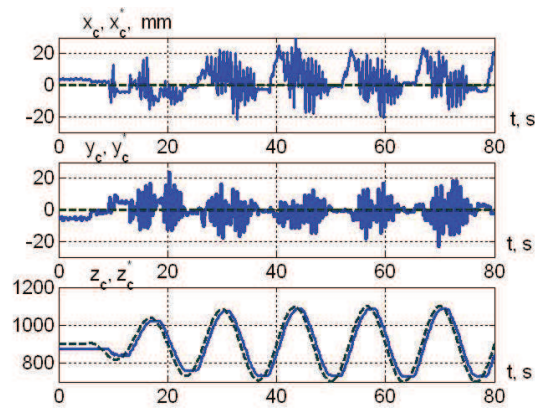


Figure 8: Experimental results. On-off logic control. Platform translational coordinates vs t . Solid line – actual value, dashed line – desired value.

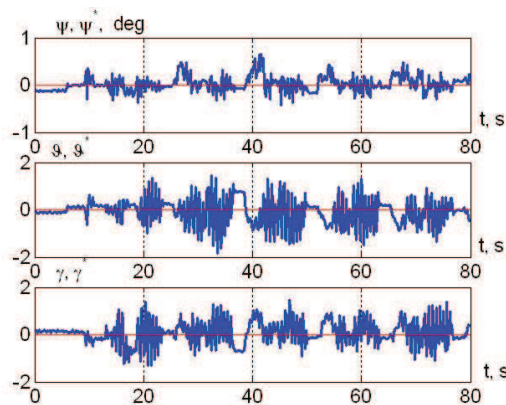


Figure 9: Experimental results. On-off logic control. Platform angular coordinates vs t .

Acknowledgment

This work was supported by Russian Scientific Foundation (project 14-21-00041) and Saint-Petersburg State University.

References

- [1] Wang, X. and Kim, C.K.-H. Improved control of pneumatic lumber-handling systems. *IEEE Trans. Control Syst. Technol.* **9** (3) (2001) 458–472.
- [2] Richardson, R., Plummer, A. and Brown M. Self-tuning control of a low-friction pneumatic actuator under the influence of gravity. *IEEE Trans. Control Syst. Technol.* **9** (2) (2001) 330–334.
- [3] Chillari, S., Guccione, S. and Muscato G. An experimental comparison between several pneumatic position control methods. In: *Proc. 40th IEEE Conf. Decision and Control (CDC 2001)*, Orlando, Florida, USA, 2001, 1168–1173.
- [4] Yin, Y. and Wang, J. A nonlinear feedback tracking control for pneumatic cylinders and experiment study. In: *Proc. American Control Conf. (ACC 2009)*, St. Louis, MO, USA, 2009, 3476–3481.
- [5] Lin, C.-L. and Chen C.-H. Design of a dead time controller for pneumatic systems. In: *Proc. American Control Conf. (ACC 2003)*, Denver, Colorado, USA, 2003, 1715–1720.
- [6] Leonov, G. A. Strange Attractors and Classical Stability Theory. *Nonlinear Dynamics and System Theory* **8** (1) (2008) 49–96.
- [7] Dasgupta, B. and Mruthyunjaya, T. The Stewart platform manipulator: a review. *Mechanism and Machine Theory* **35** (1) (2011) 15–40.
- [8] Leonov, G., Zegzhda, S., Kuznetsov, N., Tovstik, P., Tovstik, T. and Yushkov, M. Motion of a solid driven by six rods of variable length. *Doklady Physics* **59** (3) (2014) 153–157.
- [9] Andrievsky, B., Kazunin, D., Kuznetsov, N., Kuznetsova, O., Leonov, G. and Seledzhi, S. Modeling, simulation and control of pneumatically actuated Stewart platform with input quantization. In: *European Modelling Symposium EMS2014*, Pisa, Italy, 2014.
- [10] Gerc, E. and Krejcin, G. *Raschoet Pnevmoprivodov. Spravochnoe Posobie (Pneumatic Actuators Design. A Handbook)*. Mashinostroenie, Moscow, 1975 (in Russian).
- [11] Harris, P.G., O'Donnell, G.E. and Whelan T. Modelling and identification of industrial pneumatic drive system. *Int. J. Adv. Manuf. Technol.* **58** (2012) 1075–1086.
- [12] Andrievsky, B., Kazunin, D.V., Kostygova, D.M., Kuznetsov, N.V., Leonov, G.A., Lobanov, P.N. and Volkov A.A. Control of pneumatically actuated 6-DOF Stewart platform for driving simulator. In: *Proc. 19th Int. Conf. Methods and Models in Automation and Robotics (MMAR 2014)*. Miedzydroje, Poland, 2014, 663–668.
- [13] Yakubovich, V., Leonov, G. and Gelig A. *Stability of Stationary Sets in Control Systems with Discontinuous Nonlinearities*. Singapore, World Scientific, 2004.
- [14] Utkin, V. *Sliding Modes in Control and Optimization*. Springer-Verlag, 1992.
- [15] Leonov, G. A. and Shumafov, M.M. Stabilization of Controllable Linear Systems. *Nonlinear Dynamics and System Theory* **10** (3) (2010) 235–268.
- [16] Moreau, R., Pham, M.T., Tavakoli, M., Le, M.Q. and Redarce, T. Sliding-mode bilateral teleoperation control design for master–slave pneumatic servosystems. *Control Engineering Practice* **20** (2012) 584–597.
- [17] Harib, K. Srinivasan, K. Kinematic and dynamic analysis of Stewart platform-based machine tool structures. *Robotica* **21** (2003) 541–554.